Quantum stirring in low-dimensional devices

Itamar Sela and Doron Cohen

Department of Physics, Ben-Gurion University, Beer-Sheva 84005, Israel

A circulating current can be induced in the Fermi sea by displacing a scatterer or more generally by integrating a quantum pump into a closed circuit. The induced current may have either the same or the opposite sense with respect to the "pushing" direction of the pump. We work out explicit expressions for the associated geometric conductance using the Kubo-Dirac monopole picture and illuminate the connection with the theory of adiabatic passage in multiple path geometry.

I. INTRODUCTION

The question "how much charge is transported due to an adiabatic translation of a scatterer" has been raised in the context of an open geometry in Ref. 1. The scatterer is a potential barrier whose location $x=X_1$ and transmission $g_X=g(X_2)$ at the Fermi energy are determined by gate controlled parameters X_1 and X_2. For the single mode "wire" in Fig. 1(a), using the Buttiker-Thomas-Pretre (BPT) formalism,[2,3] one obtains the following result:

$$Q = (1 - g_X)\frac{e}{\pi}k_F \Delta X_1, \tag{1}$$

where $k_F = (2\mathbf{m}E_F)^{1/2}$ is the Fermi momentum and ΔX_1 is the translation distance of the scatterer. Reference 1 has referred to this transport mechanism as "snow plow" and pointed out that it should be regarded as the prototype example for quantum pumping: a full pumping cycle [Fig. 2(a)] would consist of translating the scatterer to the right, shrinking its "size," pulling it back to the left, and restoring its original size.

Quantum stirring[4,5] is the operation of inducing a dc circulating by means of ac periodic driving. This is naturally achieved by integrating a quantum pump in a closed circuit.[6–8] In particular Refs. 4 and 5 have considered the same adiabatic snow plow mechanism as described above and obtained for the model system in Fig. 1(b) the following result:

$$Q = \left[\frac{(1 - g_X)g_V}{g_X + g_V - 2g_X g_V}\right]\frac{e}{\pi}k_F \Delta X_1, \tag{2}$$

where g_V is the transmission of the ring segment that does not include the moving scatterer, as defined by its Landauer conductance if it was connected to reservoirs.

Equation (2) is "classical" in the Boltzmann sense because in its derivation the interference within the ring is ignored. The purpose of the present study is to derive quantum results for the stirring in a low-dimensional device, where quantum mechanics has the most dramatic consequences. In particular we would like to illuminate the possibility of having a counterstirring effect: by "pushing" the particles (say) anticlockwise, one can induce a circulating current in the counterintuitive (clockwise) direction.

II. OUTLINE

As a preliminary stage we provide a simple pedagogical explanation of the counterstirring effect by regarding the "pushing stage" of the pumping cycle as an adiabatic passage in multiple path geometry.[9] For the actual analysis in the general case we use the Kubo-Dirac monopole picture of Ref. 10. Within this framework the pumped charge Q is determined by the flux of a $\boldsymbol{B}(X)$ field which is identified as the Berry-Kubo curvature.[11–13] We study both analytically and numerically how this field looks like. The results are illustrated in Figs. 2–4. Summing the contributions of all the occupied levels we get expressions for the geometric conductance G. Integrating over a full pumping cycle we get results for Q.

We derive practical estimates for the stirring which is induced due to the translation of either small ($g_X \sim 1$) or a large ($g_X \ll 1$) scatterer, including the possibility of having $g_X \sim g_V$. The dependence of Q on the size of the scatterer is plotted in Fig. 5, where it is contrasted with the classical expectation and compared with the analytical approximations. In Sec. XIII we refer to the experimental measurement aspect.

III. COUNTERSTIRRING EFFECT

The essence of the counterstirring effect can be understood without the Kubo-Dirac monopole picture by adopting the "splitting ratio" concept of Ref. 9. Referring to Fig. 1(b) the translation of the scatterer to the right is effectively like lowering the potential floor in the left bond and raising the potential floor in the right bond. This induces an adiabatic passage of a particle from the right to the left. The particle has two possible ways to make the passage: either via the V
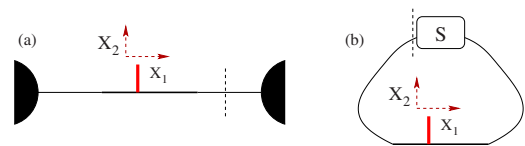

FIG. 1. (Color online) In the case of an open geometry the pumping device is connected between two unbiased reservoirs [panel (a)], while in the present study it is integrated into a ring [panel (b)]. The induced current is measured through a section indicated by a dashed line. See the text for further details.
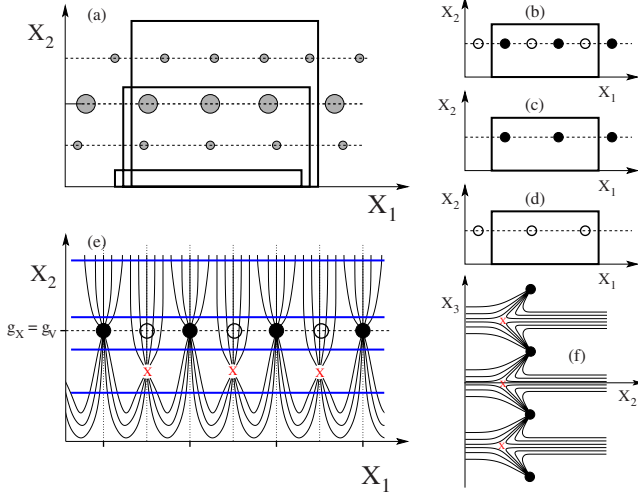
FIG. 2. (Color online) (a) Three representative pumping cycles. Several sets of Dirac monopoles may have nonzero weight depending on the occupation. Panel (b) is for single level occupation where two sets have nonzero weight, while either (c) or (d) are for zero-temperature Fermi occupation. Filled (hollow) circles indicate in (off)-plane monopoles. Panels (e) and (f) give a detailed illustration of the associated **B** field, as implied by the numerical findings of Figs. 3 and 4. The X_1 tick marks in (e) are half de Broglie spaced, while the horizontal blue lines are paths for which numerical results are presented in Figs. 3 and 4.

barrier (coupling W_{12}^V) or via the X barrier (coupling W_{12}^X). The splitting ratio determines the fraction of the current that goes via the V barrier,

$$\lambda(X_2) = \frac{W_{12}^V}{W_{12}^V + W_{12}^X} = \frac{\sqrt{g_V}}{\sqrt{g_V} \pm \sqrt{g_X}}, \quad (3)$$

where the last equality is based on the analysis in Ref. 6. If W_{12} were the classical rate of the transition, we would have $0 < \lambda < 1$ and the current would flow in accordance with our classical intuition. However W_{12}^V and W_{12}^X are *real* amplitudes that might have opposite signs if an odd level crosses an even level. Consequently if $|W_{12}^X| > |W_{12}^V|$ we get $\lambda < 0$ which implies that a circulating current is induced in the counterintuitive (clockwise) direction. This does not come in any contradiction with the observation that the net transport (summing over both barriers) is still from right to left.

IV. MODEL HAMILTONIAN

Our model is a one-dimensional (1D) coherent ring with a fixed scatterer and a controlled scatterer. The fixed scatterer is some potential barrier $V(x)$ and the controlled scatterer is modeled as a delta function whose position and transmission are determined by the control parameters X_1 and X_2. The one-particle Hamiltonian is

$$\mathcal{H} = \frac{1}{2\mathbf{m}}\hat{p}^2 + V(\hat{x}) + X_2(t)\delta[\hat{x} - X_1(t)], \quad (4)$$

with periodic boundary conditions over $x \in [-L/2, L/2]$ so as to have a ring geometry. Below we further assume that
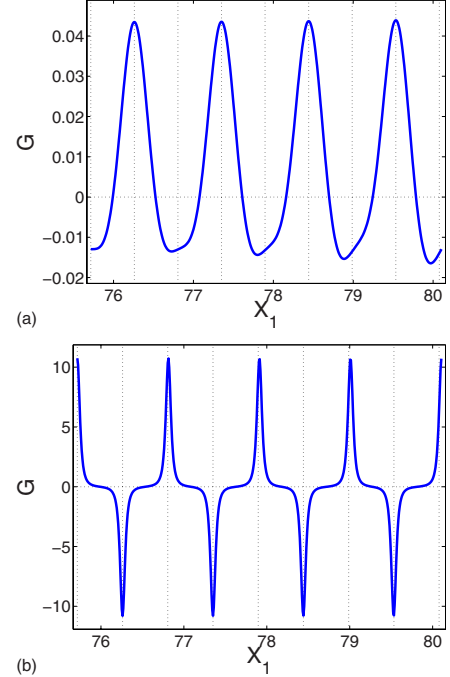

FIG. 3. (Color online) The conductance $G = G^{31}$ of Eq. (10) is numerically calculated for a ring of length $L = 151.43$ with $V(x) = U\delta(x)$, where $U \sim 10$. We consider single level occupation $n = 138$. At this energy $g_V = 0.06$. The upper (lower) panel is for translation of a very small (large) scatterer with $g_X = 0.98$ ($g_X = 8 \times 10^{-8}$) corresponding to the lower (upper) horizontal blue paths that are indicated in Fig. 2(e) (same X_1 axis).

both bonds are of similar length ($L - X_1 \sim X_1 \sim L/2$). The current is measured through a section $x = x_0 = +0$ at the fixed barrier, and accordingly
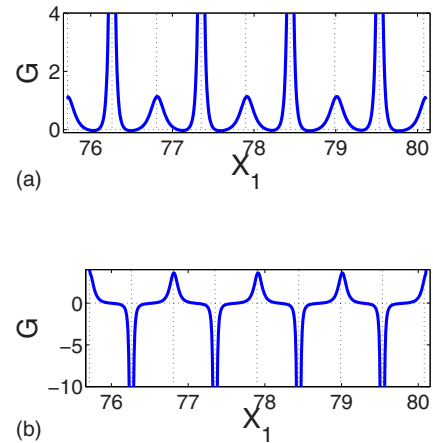

FIG. 4. (Color online) Additional plots of the conductance G as calculated in the previous figure. The upper (lower) panel is for translation of a scatterer with $g_X = 0.20$ ($g_X = 0.03$) corresponding to the horizontal blue paths in Fig. 2(e) that go below (above) the $g_X = g_V$ axis. Note that the large peaks are positive (negative) while the small positive peaks switch sign only when the scatterer is lowered further. This indicates that the field lines bend in the X_3 direction, as illustrated in Fig. 2(f).

$$\mathcal{I} = \frac{e}{2\mathbf{m}}[\hat{p}\,\delta(\hat{x} - x_0) + \delta(\hat{x} - x_0)\hat{p}]. \qquad (5)$$

We also define generalized forces which are associated with the control parameters

$$\mathcal{F}^1 = -(\partial\mathcal{H}/\partial X_1) = X_2\delta'(\hat{x} - X_1), \qquad (6)$$

$$\mathcal{F}^2 = -(\partial\mathcal{H}/\partial X_2) = -\delta(\hat{x} - X_1). \qquad (7)$$

For practical use it is more convenient to describe the fixed scatterer by its scattering matrix, which can be written as

$$S_V = e^{i\gamma_V}\begin{pmatrix} -i\sqrt{1-g_V}\,e^{i\alpha_V} & \sqrt{g_V} \\ \sqrt{g_V} & -i\sqrt{1-g_V}\,e^{-i\alpha_V} \end{pmatrix}. \qquad (8)$$

We study the case when the model parameters are such that the transmission of the fixed scatterer is small ($g_V \ll 1$), the Fermi momentum is large ($k_F L \gg 1$), and the controlled scatterer is translated a distance ΔX_1 that equals several Fermi wavelengths.

V. KUBO-DIRAC PICTURE

If we were changing the flux $X_3 \equiv \Phi$ through the ring, the induced current would be given by the Ohm law $I = \langle\mathcal{I}\rangle = -G^{33}X_3$, where G^{33} is the Ohmic conductance and $-X_3$ is the electromotive force. Similarly for a variation of the parameter X_1, the current is $I = -G^{31}\dot{X}_1$, where G^{31} is called the geometric conductance. For two parameters driving one can write

$$Q = \int I\,dt = -\oint_{\text{cycle}} \mathbf{G}\cdot d\mathbf{X} = \oint \mathbf{B}\cdot d\mathbf{s}, \qquad (9)$$

where $\mathbf{G} = (G^{31}, G^{32})$, $\mathbf{X} = (X_1, X_2)$, and $d\mathbf{s} = (dX_2, -dX_1)$. For a particle that evolves adiabatically in the level n we have $G^{31} = B_2$ and $G^{32} = -B_1$ where

$$B_j^{(n)} = \sum_{m(\neq n)} \frac{2\,\text{Im}[\mathcal{I}_{nm}]\mathcal{F}_{mn}^j}{(E_m - E_n)^2}. \qquad (10)$$

In fact, (B_1, B_2) are elements of the Kubo-Berry curvature[11–13] which one can regard as a fictitious magnetic field $\vec{B} = (B_1, B_2, B_3)$ in an embedding space $X = (X_1, X_2, X_3)$. From the requirement of having well-defined Berry phase it follows that the sources of $\vec{B}(X)$, which are located at points of degeneracy, are quantized, the so-called "Dirac monopoles."

VI. X SPACE

Due to the gauge symmetry $\Phi \mapsto \Phi + 2\pi\hbar/e$ the Dirac monopoles are arranged as vertical chains [see Fig. 2(f)] [$\hbar = e = 1$]. Due to the time-reversal invariance of our $\mathcal{H}(X_1, X_2)$ it follows that a Dirac chain is either a duplication of in-plane monopole at $X_3 = 0$ or off-plane monopole at $X_3 = \pi$. Let us find an explicit formula for the (X_1, X_2) locations of these vertical chains. The equation for the adiabatic energies $E_n(X)$ is of the form $\cos(kL + \gamma) = \sqrt{g}\cos(\Phi)$, where g is the
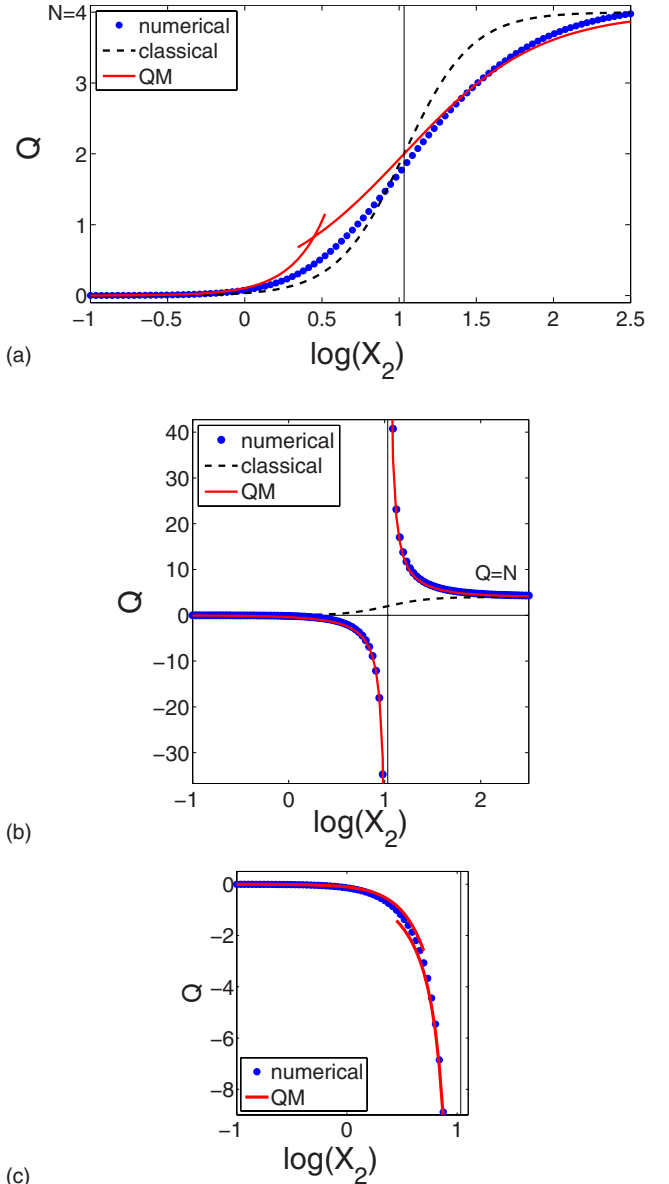

(a)

(b)

(c)

FIG. 5. (Color online) Numerical calculation of Q for zero-temperature Fermi occupation: all the levels are occupied up to $n = 137$ (upper panel) and up to $n = 138$ (lower regular and zoomed panels). The model parameters are the same as in Fig. 3. The integration was carried out along segments similar to the paths shown in Fig. 2(e) where g_X varies between $g_X = 8.30 \times 10^{-5}$ and $g_X = 0.45$. For the sake of comparison we display both the analytical classical [Eq. (2)] and quantum results [Eqs. (20) and (25)]. The value of X_2 for which $g_X = g_V$ is indicated by a vertical line.

total transmission of the ring and γ is the total phase shifts of the scatterers (the fixed scatterers plus the moving scatterer). If X_2 is such that $g_X(E; X_2) = g_V(E)$ we can always find X_1 such that the total transmission would be $g = 1$, which is the necessary condition for having a degeneracy. Together with the equation $k_E L + \gamma(E) = r\pi$ with r = integer this defines a set of energies $E^r = (k^r)^2/2\mathbf{m}$ and associated values X_2^r for which the $n = r$ level has degeneracy with the $n = r + 1$ level provided X_1 is adjusted. To be more precise r = even are in-plane ($\Phi = 0$) degeneracies, while r = odd are off-plane ($\Phi = \pi$) degen-

eracies. The X_1 locations of these degeneracies are half de Broglie wavelength apart (see Fig. 3),

$$X_1^r = \frac{\alpha_V}{2k^r} + \frac{L}{2} + \left(\left[\frac{1}{2}\right] + \text{integer}\right)\frac{\pi}{k^r}, \quad (11)$$

where the $[1/2]$ shift applies to in-plane degeneracies. The arrangement of the degeneracies in X space is illustrated in Fig. 2. For each (X_1^r, X_2^r) we have a vertical Dirac chain whose monopoles are formally like sources for the $\boldsymbol{B}$ field.

VII. FERMI OCCUPATION

If we have many-body system of $N = \Sigma_n f_n$ particles, then $\boldsymbol{B} = \Sigma_n f_n \boldsymbol{B}^{(n)}$. At finite temperature each occupied level (except $n=1$) contributes *two* sets of (X_1^r, X_2^r) chains, namely, $r = n$ and $r = n-1$, which are associated with the $E_n = E_{n\pm1}$ degeneracies. By inspection of Eq. (10), taking into account that $\mathcal{I}_{nm}$ is antisymmetric, one observes that the net contribution of the rth set of Dirac chains is $f_r - f_{r+1}$. In particular for zero-temperature Fermi occupation, the net contributions come from only *one* set of chains which is associated with the degeneracies of the last occupied level with the first non-occupied level [Figs. 2(b)–2(d)].

VIII. CLASSICAL LIMIT

At finite temperatures we can define the smeared probability distribution of the Dirac monopoles with respect to X_2 as follows:

$$f(X_2) = \overline{\sum_r [f_r - f_{r+1}]\delta(X_2 - X_2^r)}. \quad (12)$$

Disregarding fluctuations Eq. (9) implies a monotonic dependence of Q on X_2 in qualitative agreement with Eq. (2). If the expression in the square brackets of Eq. (2) was equal to $\int_0^{X_2} f(X')dX'$, it would imply a quantitative agreement as well. In order to have this quantitative agreement we have to further assume that the distribution $f(X_2)$ is determined by some chaotic dynamics in the scattering region which would imply erratic dependence of the S matrix on the energy E (see Ref. 4 for further discussion).

IX. QUANTUM LIMIT

Our interest below is in the opposite limit of zero temperature where $f(X_2)$ becomes a step function. Obviously in this limit a steplike behavior of Q versus X_2 would be a crude approximation. By inspection of Eq. (10) it follows that the result for $G \equiv G^{31} = B_2$ is very well approximated by

$$G(X_1, X_2) = \frac{2 \, \text{Im}[\mathcal{I}_{n,n+1}]\mathcal{F}_{n+1,n}^1}{(E_{n+1} - E_n)^2}, \quad (13)$$

where n is the last occupied level. This observation as well as the associated analytical results which are based on it have been verified against the exact numerical results of Figs. 3 and 4. Below we derive explicit expressions for G vs X_1 for both small and large values of X_2. Our results for Q are plotted in Fig. 5. Note that the dependence on X_1 has π/k_F

periodicity due to the X space arrangement of the monopoles, and accordingly the integration gives $Q \propto ek_F \Delta X_1/\pi$, with a prefactor that we would like to estimate.

X. MATRIX ELEMENTS

The matrix elements of the current operator $\mathcal{I}$ and of the generalized force $\mathcal{F}^1$ are

$$\mathcal{I}_{nm} = i\frac{e}{2\boldsymbol{m}}(\partial\psi^{(n)}\psi^{(m)} - \psi^{(n)}\partial\psi^{(m)}), \quad (14)$$

$$\mathcal{F}_{mn}^1 = -X_2(\overline{\partial\psi^{(m)}}\psi^{(n)} + \overline{\partial\psi^{(n)}}\psi^{(m)})$$

$$= -\frac{1}{2\boldsymbol{m}}[\partial\psi_R^{(m)}\partial\psi_R^{(n)} - \partial\psi_L^{(m)}\partial\psi_L^{(n)}], \quad (15)$$

where $\overline{\partial\psi} = 1/2(\partial\psi_L + \partial\psi_R)$ is the average derivative on the left and right sides of the delta barrier, and the second expression for $\mathcal{F}_{nm}^1$ was obtained by using the matching conditions across the delta barrier. The wave function is written as $\psi(x) = C\sin(\varphi + kx)$. We found that a very good approximation for $\mathcal{I}_{nm}$ with $m = n+1$ is

$$\mathcal{I}_{nm} = \pm ie\frac{v_F}{L}\sqrt{g_V}, \quad (16)$$

where the $+$ $(-)$ sign is for n=even (odd) and $v_F = k_F/\boldsymbol{m}$ is the velocity in the energy range of interest. For the calculation of $\mathcal{F}_{mn}^1$ and $E_m - E_n$ we have to distinguish between the two cases of small/large scatter. This means the small/large X_2 regimes where $g_X \sim 1$ or $\ll 1$.

XI. TRANSLATING A SMALL SCATTERER

If the controlled scatterer is small, we treat it as a perturbation. For the energy splitting we get

$$E_m - E_n \approx \frac{\pi}{L}v_F \mp \frac{2}{L}X_2\cos(2k_FX_1), \quad (17)$$

where for notational convenience we take X_1^r as the new origin. After some further algebra we get

$$\mathcal{F}_{mn}^1 = \pm X_2\frac{2k_F}{L}\cos(2k_FX_1) + X_2\frac{\pi}{L^2}, \quad (18)$$

where the $\pm$ sign is as in Eq. (16). The conductance can be written as

$$G = \frac{e}{\pi}k_F\sum_{\nu=0}^{\infty}\mathcal{G}_\nu\cos(\nu2k_FX_1), \quad (19)$$

where the coefficients of the leading non-negligible terms [the small parameter being $(1-g_X)/g_X$] are

$$\mathcal{G}_0 = \pm 2\sqrt{g_V}\left(\frac{1}{k_FL}\sqrt{\frac{1-g_X}{g_X}} + \frac{4}{\pi^2}\frac{1-g_X}{g_X}\right), \quad (20)$$

$$\mathcal{G}_1 = \frac{2}{\pi}\sqrt{g_V}\left(\frac{4}{k_FL}\frac{1-g_X}{g_X} + 2\sqrt{\frac{1-g_X}{g_X}}\right). \quad (21)$$

Upon integration we get $Q = -e\mathcal{G}_0$ per half Fermi wavelength displacement of the scatterer.

XII. TRANSLATING A LARGE SCATTERER

If the controlled scatterer is large, most of the charge transfer is induced during the avoided crossings (sharp peaks in Fig. 3, lower panel). Consequently we use the two level approximation scheme in Ref. 6 with $m=n+1$ leading to the following results:

$$E_m - E_n = \frac{2}{L} v_F |\boldsymbol{R}|, \tag{22}$$

$$\mathcal{F}_{mn}^1 = \pm \frac{2}{L} \mathbf{m} v_F^2 \frac{R_2}{|\boldsymbol{R}|}, \tag{23}$$

where the $\pm$ sign is as in Eq. (16) and the dimensionless distance in X space from the degeneracy point is

$$\boldsymbol{R} = \left(2k_F (X_1 - X_1^r), \frac{\sqrt{g_V}}{\lambda(X_2)} \right), \tag{24}$$

Accordingly the conductance is

$$G = e \frac{k_F}{\sqrt{g_V}} \frac{R_2}{|\boldsymbol{R}|^3}. \tag{25}$$

Integrating over X_1 we get $Q = e\lambda(X_2)$ per half Fermi wavelength displacement of the scatterer, as expected from the splitting ratio argument.

XIII. SUMMARY

The integration of a two-terminal quantum pump in a closed circuit is not a straightforward procedure. Due to interference the pumped charge Q would not be the same as in the Landauer/BPT setup, and even the sense of the induced current might be reversed. The most dramatic consequences would be observed in low-dimensional devices. For this reason we have analyzed in this paper the prototype problem of pushing a current by translating a scatterer in a single mode wire. We have obtained explicit results for the $\boldsymbol{B}$ field, which determines the geometric conductance G and consequently the Q of a closed pumping cycle. We also illuminated the counterstirring effect using the splitting ratio concept of adiabatic passage in multiple path geometry.

A few words are in order regarding the measurement procedure and the experimental relevance. It should be clear that to measure current in a closed circuit requires special techniques.[14–16] These techniques are typically used in order to measure persistent currents, which are zero-order (conservative) effect, while in the present paper we were discussing driven currents, which are a first-order (geometric) effect. It is of course also possible to measure the dissipative conductance (as in Ref. 14). During the measurement the coupling to the system should be small. These are so-called *weak measurement* conditions. More ambitious would be to measure the counting statistics, i.e., also the second moment of Q as discussed in Refs. 9 and 17 which is completely analogous to the discussion of noise measurements in open systems.[18,19] Finally it should be pointed out that the formalism above, and hence the results, might apply to experiments with superconducting circuits (see Ref. 8).

[1] J. E. Avron, A. Elgart, G. M. Graf, and L. Sadun, Phys. Rev. B **62**, R10618 (2000).

[2] M. Buttiker, H. Thomas, and A. Pretre, Z. Phys. B: Condens. Matter **94**, 133 (1994).

[3] P. W. Brouwer, Phys. Rev. B **58**, R10135 (1998).

[4] G. Rosenberg and D. Cohen, J. Phys. A **39**, 2287 (2006).

[5] D. Cohen, T. Kottos, and H. Schanz, Phys. Rev. E **71**, 035202(R) (2005).

[6] I. Sela and D. Cohen, J. Phys. A **39**, 3575 (2006).

[7] M. Moskalets and M. Büttiker, Phys. Rev. B **68**, 161311(R) (2003).

[8] M. Mottonen, J. P. Pekola, J. J. Vartiainen, V. Brosco, and F. W. J. Hekking, Phys. Rev. B **73**, 214523 (2006).

[9] M. Chuchem and D. Cohen, J. Phys. A **41**, 075302 (2008).

[10] D. Cohen, Phys. Rev. B **68**, 155303 (2003).

[11] M. V. Berry, Proc. R. Soc. London, Ser. A **392**, 45 (1984).

[12] J. E. Avron, A. Raveh, and B. Zur, Rev. Mod. Phys. **60**, 873 (1988).

[13] M. V. Berry and J. M. Robbins, Proc. R. Soc. London, Ser. A **442**, 659 (1993).

[14] Measurements of currents in arrays of closed rings are described by B. Reulet, M. Ramin, H. Bouchiat, and D. Mailly, Phys. Rev. Lett. **75**, 124 (1995).

[15] Measurements of currents in individual closed rings using SQUID is described in: N. C. Koshnick, H. Bluhm, M. E. Huber, and K. A. Moler, Science **318**, 1440 (2007).

[16] A micromechanical cantilever technique for measuring currents in closed rings is described by A. C. Bleszynski-Jayich, W. E. Shanks, R. Ilic, and J. G. E. Harris, arXiv:0710.5259 (unpublished).

[17] M. Chuchem and D. Cohen, Phys. Rev. A **77**, 012109 (2008).

[18] L. S. Levitov and G. B. Lesovik, JETP Lett. **58**, 230 (1993).

[19] Y. V. Nazarov and M. Kindermann, Eur. Phys. J. B **35**, 413 (2003).